# A Verification of Grounding Structure for Short-Circuited Stub for Wideband Bandpass Filter in LMT-FINER
## - Demonstrating Superior Tolerance to Surface Finishes -

Jiashen WENG† Taiyo USHIYAMA† Satoshi ONO† and Takeshi SAKAI†

†Graduate School of Informatics and Engineering, The University of Electro-Communications 1-5-1 Chofugaoka, Chofu, Tokyo, 182-8585 Japan

E-mail: †{jiashen.weng, ono.satoshi}@ uec.ac.jp

**Abstract** We evaluated grounding structures and surface finishes for short-circuited stub wideband bandpass filters (BPFs) designed for Large Millimeter Telescope Far Infrared Nebular Emission Receiver (LMT-FINER). Three grounding structures were tested: circular via holes (Type 1), rectangular stubs with vias (Type 2), and combining top-layer ground planes, wide low-impedance stub terminations, and stitching vias at impedance boundaries (Type 3). Each structure was tested with three surface finishes (untreated, OSP-treated, and ENIG-treated). The results showed that Type 3 achieved the closest match to the designed passband specifications while demonstrating superior tolerance to surface finish variations compared to conventional approaches. These findings provide crucial design points for short-circuited stub wideband BPF manufacturing.

**Keyword** Wideband bandpass filter, short-circuit stub, grounding structures, surface finishes

## 1. Introduction

The LMT-FINER project aims to install a 120-350 GHz heterodyne receiver on the Large Millimeter Telescope in Mexico, requiring an anti-aliasing bandpass filter (BPF) operating at 10.24-20.48 GHz with 66.7% fractional bandwidth [1]. This wideband BPF demands precise cutoff frequency control, which presents significant design challenges.

While short-circuited stub BPFs offer straightforward wideband implementations [2,3], achieving accurate cutoff frequencies above 10 GHz is challenging due to parasitic effects from via structures [4] and manufacturing variations [5,6]. Recent studies have proposed alternative grounding structures including radial stubs [7] and modified via geometries [8,9], but systematic comparisons at X-, Ku-, and K-band frequencies remain lacking. Additionally, PCB surface finishes required for environmental durability (Organic Solderability Preservative (OSP), Electroless Nickel Immersion Gold (ENIG), and so on) affect both insertion loss and cutoff frequency [10-13]. In the case of a grounded coplanar waveguide with surface finishes, detailed experimental verification results were provided [14]. Also, it showed the difference in frequency characteristics by arranging vias. These results significantly showed the effect of surface finishes. In the present work, we showed the combined effects, which are via arrangements and surface finishes with grounding structures, against wideband filters using a microstrip line (MSL) structure with co-ground planes. It remains unexplored to the MSL structure with co-ground planes [3-6]. Specifically, this paper examines how the joint effects of grounding structures and surface finishes impact BPF frequency characteristics. We introduce a stitching via structure (Type 3) and compare it with conventional circular (Type 1) and rectangular (Type 2) stub designs under three surface finishes: untreated, OSP, and ENIG. Our experimental results provide practical design points for achieving cutoff frequency requirements in the 10.24-20.48 GHz range.

## 2. Substrate Materials, Surface finish And Stub Grounding structures

### 2.1. Substrate Material Characteristics

Table 1 shows the prototype printed circuit board (PCB) material properties. We used xCH-3008 substrate (Chukoh Chemical Industries, t = 0.254 mm), a PTFE/glass cloth composite with low dielectric constant and loss tangent that minimizes transmission line losses [6]

Table 1 Substrate material characteristics [15]

| Substrate material | xCH-3008 (t=0.254mm) |
|---|---|
| Dielectric constant $\varepsilon_r$ | 3.05 @13GHz (Measured data) |
| Dielectric tangent $\tan\delta$ | 0.0012 @13GHz (Measured data) |

### 2.2. Surface finish Layer Structure

As shown in Figure 1, we fabricated prototype PCBs with the same surface finish on both sides: (a) with OSP-treated copper foil surface finish, and (b) with ENIG surface finish.

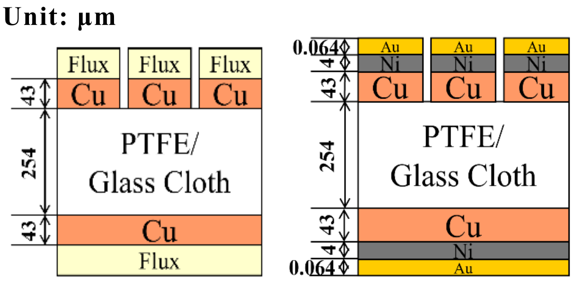


(a) (b)

Fig.1. Layer structure of (a) OSP-treated substrates, (b) ENIG finish.

### 2.3. Design Of Grounding Structures

In this study, we investigated the following three grounding structures:

Type 1 (Circular stub): This is the conventional via hole grounding structure shown in Figure 2. It connects to the ground plane through a through-hole via using a circular stub pattern. A via pad corresponds to a via hole.

Type 2 (Rectangular stub): This is also one of the conventional grounding structures. It aims to improve the grounding effect by using a rectangular stub pattern, which is shown in Figure 3. Because of the two parallel vias shown in Fig.3, the equivalent series resistances (ESRs) and equivalent series inductances (ESLs) are reduced to approximately half of those of Type 1[4].

Type 3 (Stitching via structure): This proposed structure combines three elements: (1) top-layer ground planes in the microstrip filter, (2) wide low-impedance sections at stub ends creating clear impedance boundaries, and (3) multiple stitching vias at these boundaries. This combination minimizes parasitic inductance and improves grounding effectiveness above 10 GHz [4].

## 3. Design Of Wideband BPF

### 3.1. Design of Ninth-Order Wideband BPF

The ninth-order BPF design methodology was based on [3]. To verify that the specified bandwidth could be achieved in practice, we selected a ninth-order design. We used 2.92 mm coaxial end-launch connectors to avoid performance degradation from center pin soldering. Therefore, 50 Ω grounded coplanar waveguide (GCPW) structures were employed as input/output feed lines. The ninth-order Chebyshev BPFs were configured using a microstrip line structure. The design specifications are shown in Table 2.

Table 2 Design specifications for wideband BPF.

| | |
|---|---|
| Center Frequency ($f_0$) | 15.36 GHz |
| Fractional bandwidth (FBW) | 66.7% |
| Passband ripple | < 3 dB |

In the design, the characteristic impedance of each stub was optimized using circuit simulation, and then the physical structure was determined using the 3D electromagnetic simulator HFSS.

Figures 2, 3, and 4 show the circuit patterns of wideband BPFs using different grounding structures. The simulation results based on untreated copper foil surfaces are shown in Figure 5.

In this design, the use of a thin substrate thickness of 0.254 mm resulted in the optimization of via characteristics. According to [4], the substrate thickness is the parameter that has the most significant influence on via inductance. However, even for a substrate thickness of t=0.254 mm, it is shown in [4] that the via inductance is significantly reduced compared to thicker substrates. This low inductance characteristic enabled the realization of sufficient short-circuit characteristics even in end stubs using a single via.

Table 3 compares the EM simulated responses for untreated copper. The simulation results show that the Type 1 pattern best matches the design specifications for the passband. In Table 3, $f_l$, $f_u$, BW, and IL-max show the lowest and the highest cutoff frequencies, Bandwidth ($f_l$-$f_u$), and maximum insertion loss in the in-band of BPF, respectively.

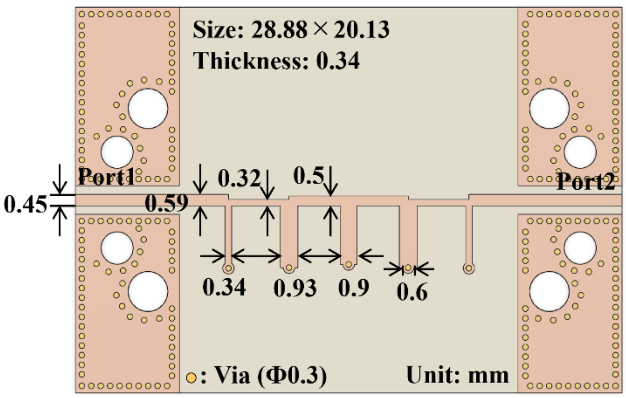


Fig.2.Type 1 circuit pattern

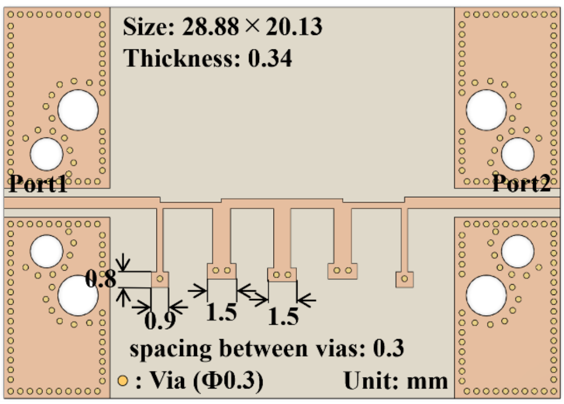


Fig.3.Type 2 circuit pattern

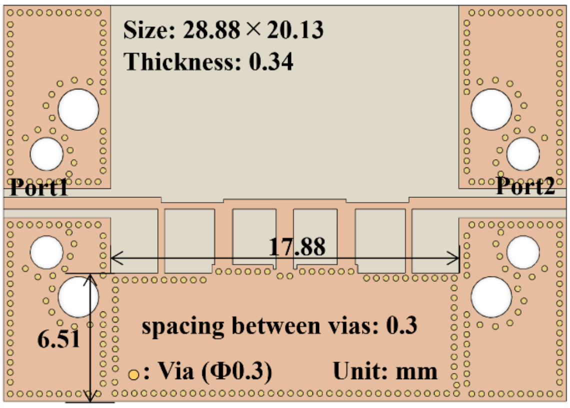


Fig.4.Type 3 circuit pattern

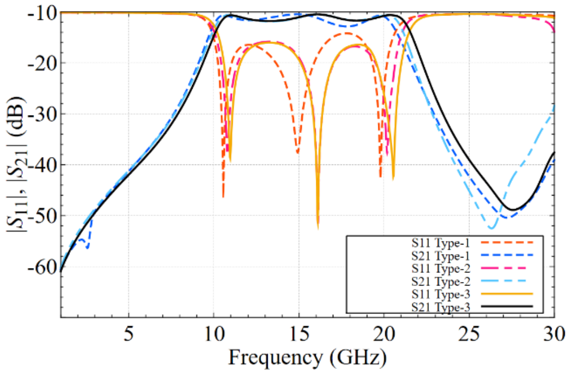


Fig.5. Simulated responses of the Type 1, Type 2, and Type 3.

Table 3 Each characteristic for BPFs(sim).

| | Type 1 | Type 2 | Type 3 |
|---|---|---|---|
| $f_0$(GHz) | 15.23 | 15.52 | 15.80 |
| $f_l$(GHz) | 10.04 | 10.28 | 10.45 |
| $f_U$(GHz) | 20.42 | 20.76 | 21.15 |
| BW(GHz) | 10.38 | 10.48 | 10.70 |
| FBW (%) | 68.2 | 67.5 | 67.7 |
| IL-max(dB) | 2.85 | 1.65 | 1.71 |

## 4. Experimental Results and Analysis

Based on the simulation results, we fabricated a total of nine prototype PCBs with combinations of three grounding structures and three surface finishes.

Measurements were performed using a vector network analyzer, which is an Agilent Technologies E8363C. A frequency range of 1-30 GHz was set. This section presents the measurement results and analyzes the effects of both grounding structures and surface finishes on filter performance.

### 4.1. Measurement Result

Figures 6 and 7 show the fabricated BPFs and measured frequency characteristics for different grounding structures and surface finishes.

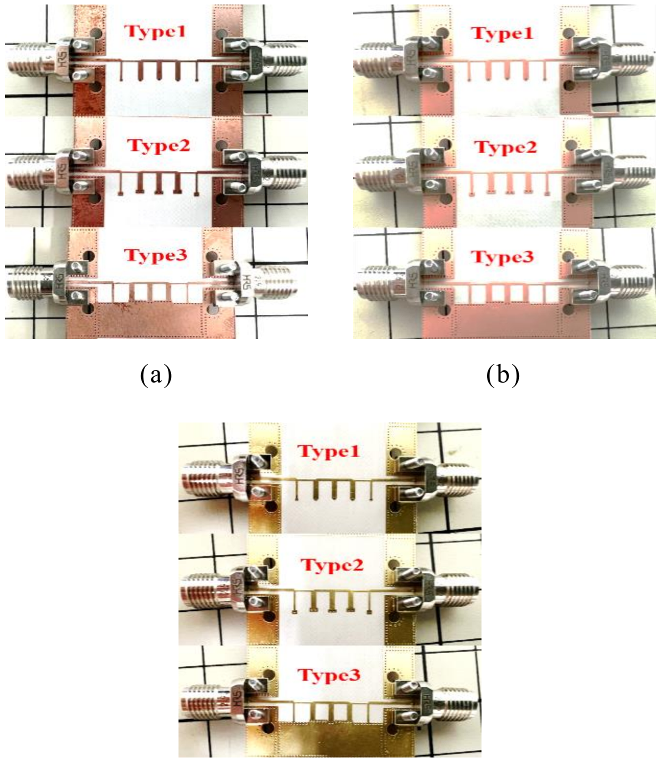


(c)

Fig.6. Fabricated BPFs of (a) untreated (b) OSP-treated (c) ENIG-treated

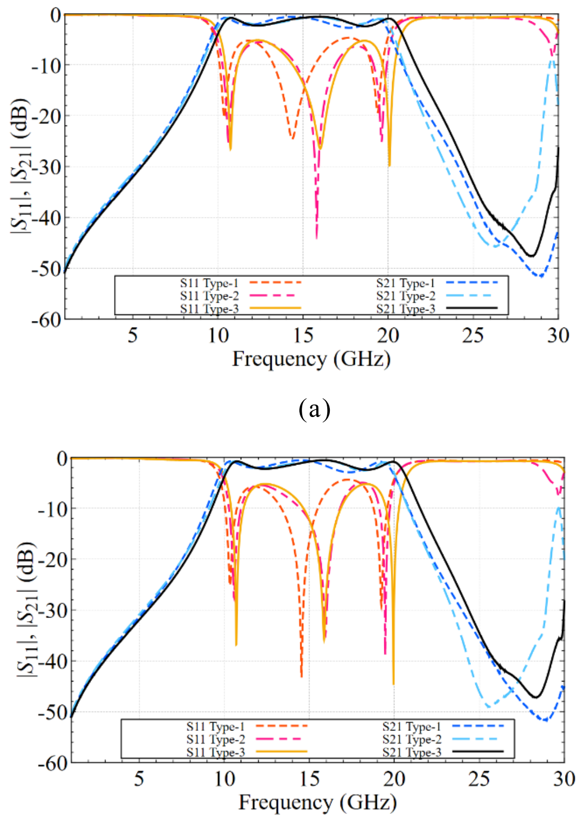


(b)

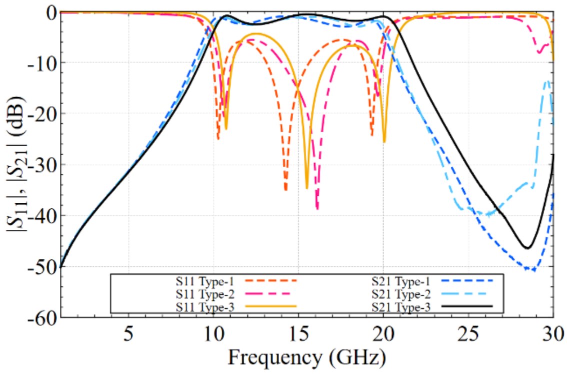


(c)

Fig.7. The frequency characteristics of each grounding structure for (a)untreated copper foil, (b) OSP-treated copper foil, (c) ENIG-treated copper foil.

### 4.2. Center Frequency Response Analysis

The center frequency $f_o$ is a critical parameter determining the filter's operating band. Table 4 shows the measured center frequencies for all nine configurations.

Table 4. $f_o$ measurements and deviations

| | Untreated (GHz) | OSP (GHz) | ENIG (GHz) | Target[1] Deviation (GHz) |
|---|---|---|---|---|
| Type1 | 14.88 | 14.83 | 14.75 | -0.61 to -0.48 |
| Type2 | 15.07 | 14.95 | 15.02 | -0.41 to -0.29 |
| Type3 | 15.41 | 15.34 | 15.39 | +0.05 to -0.02 |

[1]Design target: 15.36 GHz

The Type 3 structure exhibited the least variation across all surface finishes, showing a deviation of only -0.02 to +0.05 GHz from the target. This superior stability can be attributed to the distributed grounding mechanism, which effectively minimizes parasitic inductance variations [4].

### 4.3. Cutoff Frequency Characteristics

The cutoff frequency of the BPF changes depending on the surface finish [6]. As shown in Tables 5 and 6, Type 3 demonstrated exceptional stability across all surface finishes.

Table 5. $f_l$ measurements and achievement

| | Untreated (GHz) | OSP (GHz) | ENIG (GHz) | Target Achievement[2] (%) |
|---|---|---|---|---|
| Type1 | 9.88 | 9.84 | 9.78 | 95.5~96.5 |
| Type2 | 10.1 | 10.08 | 10.06 | 98.2~98.6 |
| Type3 | 10.24 | 10.22 | 10.24 | 99.8~100.0 |

[2]Target:10.24 GHz

Table 6. $f_u$ measurements and achievement

| | Untreated (GHz) | OSP (GHz) | ENIG (GHz) | Target Achievement[3] (%) |
|---|---|---|---|---|
| Type1 | 19.87 | 19.82 | 19.72 | 96.3~97.0 |
| Type2 | 20.03 | 19.82 | 19.98 | 96.8~97.8 |
| Type3 | 20.57 | 20.46 | 20.54 | 99.9~100.4 |

[3]Target:20.48 GHz

Remarkably, Type 3 maintained $f_l$ at exactly 10.24 GHz for both untreated and ENIG configurations, achieving 100% target compliance. This stability indicates that the stitching via structure provides a robust ground reference that is virtually immune to surface finish variations at lower frequencies.

### 4.4. Bandwidth and Fractional Bandwidth Analysis

Tables 7 and 8 show the measured bandwidths and fractional bandwidth, demonstrating Type 3's superior achievement of the design specification.

Table 7. BW measurements and deviations

| | Untreated (GHz) | OSP (GHz) | ENIG (GHz) | Target[4] Deviation (GHz) |
|---|---|---|---|---|
| Type1 | 9.99 | 9.98 | 9.94 | -0.30 to -0.25 |
| Type2 | 9.93 | 9.74 | 9.92 | -0.50 to -0.31 |
| Type3 | 10.33 | 10.24 | 10.3 | 0.00 to +0.09 |

[4]Target: 10.24 GHz

Table 8. FBW measurements and deviations

| | Untreated (%) | OSP (%) | ENIG (%) | Target[5] Deviation (%) |
|---|---|---|---|---|
| Type1 | 67.2 | 67.3 | 67.4 | +0.50 to +0.70 |
| Type2 | 65.9 | 65.2 | 66 | -1.50 to -0.70 |
| Type3 | 67.1 | 66.8 | 66.9 | +0.10 to +0.40 |

[5]Target: 66.7%

Type 3 with OSP achieved perfect bandwidth matching (10.24 GHz) while maintaining excellent performance across other treatments. Additionally, Type 3 achieved the optimal balance between absolute and relative specifications.

Comparing simulation results with measurements reveals that while Type 1 showed the best agreement in simulation, Type 3 demonstrated superior performance in practice. This discrepancy stems from the incomplete modeling of via parasitic effects in the simulation. The single via in Type 1 introduces concentrated parasitic inductance that varies with manufacturing tolerances, whereas Type 3's distributed vias create multiple parallel paths that effectively average out these variations [4].

Among the three grounding structures, Type 3 consistently achieved the closest match to design specifications across all surface finishes. The distributed grounding mechanism effectively minimizes parasitic inductance variations, making it the optimal choice for wideband BPF implementation in the 10.24-20.48 GHz range.

### 4.5. Insertion Loss Performance

Insertion loss directly impacts system efficiency Table 9 demonstrates Type 3's exceptional loss stability across surface finishes.

Table 9. Maximum Insertion Loss in Passband

| | Untreated (dB) | OSP (dB) | ENIG (dB) | Maximum Degradation[6] (dB) |
|---|---|---|---|---|
| Type1 | 2.74 | 2.93 | 2.96 | 0.22 |
| Type2 | 1.97 | 2.61 | 2.95 | 0.98 |
| Type3 | 2.43 | 2.44 | 2.48 | 0.05 |

[6]Degradation: Compared to untreated

Type 3 exhibited only 0.05 dB degradation (2.1% relative change) across all surface finishes, compared to 0.22 dB (8.0%) for Type 1 and 0.98 dB (49.7%) for Type 2. The distributed grounding through multiple vias creates parallel current paths that effectively average out local variations in surface conductivity, resulting in more stable overall performance.

## 5. Conclusion

In this study, we systematically evaluated three grounding structures and three surface finishes for ninth-order wideband BPFs designed for the LMT-FINER project. Our novel stitching via structure (Type 3) demonstrated superior performance compared to conventional approaches. Based on comprehensive experimental results, we provide the following design points:

1. Grounding structure selection: The novel stitching via structure (Type 3) should be selected for wideband BPFs in X-, Ku-, and K-bands, achieving 99.8-100% target compliance for cutoff frequencies—significantly outperforming conventional circular (Type 1) and rectangular (Type 2) structures.

2. Surface finish selection: For optimal frequency performance, untreated copper is recommended when protection is not critical. Among the surface finishes evaluated in this study, OSP treatment should be selected for bandwidth-critical applications (achieving an exact 10.24 GHz bandwidth with Type 3). At the same time, ENIG can be considered when a slightly higher insertion loss is acceptable.

These findings provide crucial design points for the LMT-FINER project and similar high-frequency applications. The novel stitching via structure offers a good solution for achieving stringent bandwidth requirements while maintaining performance stability across different surface finishes.

**Acknowledgement**

The authors are indebted to Mr. Makoto Yoshida of CDEX Corporation, who generously and gratefully provided prototype boards and shared his expertise in measurement techniques.

**References**

[1] FINER Project. (n.d.). FINER project. [Online]. Available: https://finerreceiver.github.io/ja/. [Accessed: 28-7 2025].

[2] J.S Hong, *Microstrip Filters for RF/Microwave Applications*, John Wiley SONS, INC.pp.489-495, 2011.

[3] R. Hamano, Z. Ma, M. Ohira, C.-P. Chen, and T. Anada, "Design of Ultra-Wideband Bandpass Filter using short-circuited stubs," IEICE Technical Report, vol. 114, no. 376, pp. 125-131, Dec. 2014.

[4] Eric Holzman, *Essentials of RF and Microwave Grounding*, Artech, 2006.

[5] "Non-Destructive Analysis and EM Model Tuning of PCB Signal Traces using the Beatty Standard", White Paper from DesignCon 2017, Jan. 2017.

[6] M. Yoshida, Y. Tsubaki, T. Yakabe, and S. Ono, "Evaluation of electroless Au-Pd-Au plated printed circuit boards in millimeter-wave band," IEICE Technical Report, vol.125, no. 7, MW2025-4, pp. 17-22, Apr. 2025.

[7] S. Ladan, S. Hemour, and K. Wu, "A millimeter-wave wideband microstrip RF and DC grounding," 2012 42nd European Microwave Conference, Amsterdam, Netherlands, pp. 13-16,2012.

[8] Marki Microwave, "Amplifier Grounding," Application Note, Oct. 2023. [Online]. Available: https://markimicrowave.com/assets/65410e42-e08d-41b4-80c4-feec9f8b31c6/Marki_Microwave_Amplifier_Grounding.pdf [Accessed: 28-7 2025]

[9] Runtime Rec, "How to Minimize Parasitic Effects," [Online]. Available: https://runtimerec.com/how-to-minimize-parasitic-effects/. [Accessed: 28-7 2025].

[10] O. Huber, G. Magerl, and H. Arthaber, "Impact of different surface finishes on insertion loss for microstrip resonators up to 110 GHz," 2017 IEEE Radio and Antenna Days of the Indian Ocean

(RADIO), Cape Town, South Africa, pp. 1-2, 2017.
[11] A. Ippich, "PCB Surface Finish Impact to Losses at High Frequencies," 2019 IEEE International Conference on Microwaves, Antennas, Communications and Electronic Systems (COMCAS), Tel-Aviv, Israel, pp. 1-4, 2019.
[12] B. Curran, I. Ndip, and K. -D. Lang, "A comparison of typical surface finishes on the high frequency performances of transmission lines in PCBs," 2017 IEEE 21st Workshop on Signal and Power Integrity (SPI), Lake Maggiore, Italy, pp. 1-3, 2017.
[13] D. Staiculescu, J. Laskar, J. Mendelsohn, E. Sweetman, D. Rudy, and I. Anaki, "Ni-Au surface finish effects on RF performance," 1999 IEEE MTT-S International Microwave Symposium Digest (Cat. No.99CH36282), Anaheim, CA, USA, pp. 1909-1912,1999.
[14] M. Yoshida and T. Yakabe, "Evaluation of Grounded Coplanar Waveguide with Edge Faces Plated," IEICE Technical Report, vol.124, no. 212, MW2025-99, pp. 56-61, Oct. 2024.
[15] Chukoh Chemical Industries, Ltd., "xCH-3008 CHUKOH FLO Copper-clad Laminates," Technical Datasheet, Apr. 1, 2024. [Online]. Available: https://www.chukoh.co.jp/wp-content/uploads/xCH-3008-leflet.pdf. [Accessed: 28-7 2025]